Applied Mathematical Sciences, Vol. 9, 2015, no. 27, 1311 - 1329
HIKARI Ltd, www.m-hikari.com
http://dx.doi.org/10.12988/ams.2015.513

A Double Power-Law Fit to the Computed Stellar $\log(\tau/\mathrm{y})$-$\log(m/m_\odot)$ Relation

R. Caimmi

Physics and Astronomy Department, Padua University
Vicolo Osservatorio 3/2, I-35122 Padova, Italy

Abstract

The computed $\log(\tau/\mathrm{y})$-$\log(m/m_\odot)$ relation for the stellar initial mass range, $0.6 \le m/m_\odot \le 120.0$, and the stellar initial metallicity range, $0.0004 \le Z \le 0.0500$, tabulated in an earlier attempt [14] is fitted to a good extent by a four-parameter curve, expressed by a double power-law, for assigned stellar initial metallicity, which can be reduced to a three-parameter curve, expressed by a single power-law, for the whole set of stellar initial metallicities. The relative errors, $R[\log(\tau/\mathrm{y})] = 1 - \log(\tau_{\mathrm{fit}}/\mathrm{y})/\log(\tau/\mathrm{y})$, do not exceed about 2% and 4%, respectively. The extent to which the interpolation curve, expressed by a single power-law, can be extrapolated towards both high-mass and low-mass stars, is also investigated. High-mass star lifetimes are understimated by a factor less than 2 up to $m/m_\odot = 1000$ and by a fiducial factor less than 4 up to $m/m_\odot \to +\infty$. Low-mass star lifetimes are overstimated by a factor of about 3 down to $m/m_\odot = 0.25$ and by an unacceptably large factor down to $m/m_\odot = 0.08$. The interpolation curve, expressed by a single power-law, is related (in differential form) to a generalization of the equation of the exponential decay, which could be the starting point for a theoretical interpretation. As a simple application, the star mass fraction of a single star generation with stellar initial mass function defined by a power-law, is plotted vs. the logarithmic stellar lifetime. The star mass fraction declines in time at a decreasing rate for mild stellar initial mass function and at an increasing rate for steep stellar initial mass function, where a linear trend is exhibited for a value of the exponent close to the Salpeter's value ($p_{\mathrm{lin}} \approx -2.35$).

Keywords: stars: evolution, stars: formation

1 Introduction

For isolated stars, the stellar lifetime is defined as the time needed to move from the zero-age main sequence up to the giant branch and through any subsequent giant evolution. There is no easy way to infer stellar lifetime as a function of stellar initial mass, from a selected star sample belonging to an assigned population. Accordingly, τ-m or $\log(\tau/\mathrm{y})$-$\log(m/m_\odot)$ relations, where τ is the stellar lifetime and m the stellar initial mass, are interpolation curves to the results from stellar evolution models (e.g., [10], [12]). For further details, an interested reader is addressed to recent overviews (e.g., [17]).

A systematic dependence of the $\log(\tau/\mathrm{y})$-$\log(m/m_\odot)$ relation on the stellar initial metallicity, Z, is available in tabular form within the mass range, $0.6 \le m/m_\odot \le 120.0$, and the initial metallicity range, $0.0004 \le Z \le 0.0500$, where the changes due to different initial metallicities can be neglected to a first extent [14]. Accordingly, lifetime is a strongly decreasing function of the initial mass and only weakly dependent on the initial metallicity (e.g., [19]).

Interpolating the computed $\log(\tau/\mathrm{y})$-$\log(m/m_\odot)$ relation via a simple, continuous, derivable curve, could be useful in problems where the first derivatives, $\mathrm{d}\tau/\mathrm{d}m$ or $\mathrm{d}m/\mathrm{d}\tau$, and higher order derivatives are needed, such as chemical evolution models. The current note focuses on a computed $\log(\tau/\mathrm{y})$-$\log(m/m_\odot)$ relation where the dependence of stellar lifetime on stellar initial mass and metallicity is exploited [14], aiming to the expression of four-parameter curves involving a double power-law, more specifically an exponential whose argument is, in turn, a power.

To this respect, using standard regression techniques seems to be inappropriate, in that different stellar evolution models yield different results for an assigned choice of input parameters, due to still persisting uncertainties on some physical processes, and standard regression curve procedures would be of little significance in the case under discussion. Then a different strategy must be exploited, where four "crossing" points are specified as belonging to the interpolation curve.

With regard to a fixed stellar initial metallicity, the coordinates of the crossing points can coincide with computer outputs, $[\log(m_\mathrm{U}/m_\odot), \log(\tau_\mathrm{U}/\mathrm{y})]$, U = 0, A, B, C, to be fixed as appropriate. With regard to the whole set of initial metallicities for which the results are available, the ordinates of the crossing points can be determined as average values of their counterparts related to the whole set of initial metallicities, while abscissae remain unchanged, $[\log(m_\mathrm{U}/m_\odot), \overline{\log(\tau_\mathrm{U}/\mathrm{y})}]$, U = 0, A, B, C, to be fixed as appropriate, where $\overline{\log(\tau_\mathrm{U}/\mathrm{y})} = [\log(\tau_\mathrm{U}/\mathrm{y})_1 + ... + \log(\tau_\mathrm{U}/\mathrm{y})_N]/N$ and $N = 5$ in the case under discussion [14].

Four-parameter interpolation curves, for both selected initial metallicities and the whole set of initial metallicities, are derived in section 2. The results are presented in section 3. An illustrative application is shown in section 4. The discussion and the conclusion are performed in section 5.

2 Four-parameter interpolation curves

A complete set of computed stellar lifetime within the initial mass range, $0.6 \le m/m_\odot \le 120.0$, and the initial metallicity range, $0.0004 \le Z \le 0.0500$, is available in tabular form [14]. More specifically, stellar evolution has been computed for 30 stellar initial masses, where 15 lie within the range, $0.6 \le m/m_\odot \le 2.0$, 7 within the range, $2.5 \le m/m_\odot \le 9.0$, 6 within the range, $12.0 \le m/m_\odot \le 60.0$, with the addition of $m/m_\odot = 100.0, 120.0$; initial metallicities have been fixed to $Z_1 = 0.0004$, $Z_2 = 0.0040$, $Z_3 = 0.0080$, $Z_4 = 0.0200$, $Z_5 = 0.0500$. It is worth noticing Z_4, initially conceived as solar value, is supersolar according to a recent investigation yielding $Z_\odot = 0.134$ [3].

The computed $\log(\tau/\mathrm{y})$-$\log(m/m_\odot)$ relation, listed in tabular form in an earlier attempt [14], is plotted in Fig. 1 where different symbols relate to different initial metallicities: Z_1 - crosses; Z_2 - diamonds; Z_3 - triangles; Z_4 - squares; Z_5 - saltires.

The interpolation of the results shall be performed via four-parameter curves defined as [7]:

$$y = f(x) = C_1 \exp(-C_2 x^\gamma) + C_3 \quad ; \qquad x \ge 0 \quad ; \tag{1}$$

where C_1, C_2, C_3, γ, are parameters to be determined by fitting to a good extent.

Regression curves based on standard methods, such as least squares procedure, could be of little significance in that different stellar evolution codes with same input parameters yield different results, due to still persisting uncertainties on specific details of stellar evolution theory.

For this reason, a different strategy shall be adopted, namely interpolation curves are constrained to pass through four crossing points, (x_0, y_0), (x_A, y_A), (x_B, y_B), (x_C, y_C), which implies the determination of the unknown parameters. More specifically, the substitution of the coordinates in Eq. (1) yields a system of four transcendental equations in four unknowns, C_1, C_2, C_3, γ, as:

$$y_0 = C_1 + C_3 \quad ; \qquad x_0 = 0 \quad ; \tag{2}$$

$$y_\mathrm{U} = C_1 \exp(-C_2 x_\mathrm{U}^\gamma) + C_3 \quad ; \qquad \mathrm{U} = \mathrm{A, B, C} \quad ; \tag{3}$$

where $x_0 = 0$, for convenience.

The combination of Eqs. (1) and (2) yields:

$$\frac{y - C_3}{C_1} = \frac{C_1 - y_0 + y}{C_1} = [\exp(-C_2)]^{x^\gamma} > 0 \quad ; \tag{4}$$

which is equivalent to:

$$C_2 = x^{-\gamma} \ln \frac{C_1}{C_1 - y_0 + y} \quad ; \tag{5}$$

where $C_1 < 0$ or $C_1 > y_0 - y > 0$ in the case under discussion.

The particularization of Eq. (5) to (x_U, y_U), (x_V, y_V), after performing the ratio on both sides of related equations, produces:

$$\left(\frac{x_\mathrm{V}}{x_\mathrm{U}} \right)^\gamma = \frac{\ln[(C_1 - y_0 + y_\mathrm{V})/C_1]}{\ln[(C_1 - y_0 + y_\mathrm{U})/C_1]} \quad ; \tag{6}$$

with the above mentioned restrictions for y_U, y_V, to ensure positive argument of related logarithm. In the case under discussion, both x and γ are real, which implies the ratio on the right-hand side of Eq. (6) is non negative i.e. the arguments of the logarithms are both either larger or lower than unity. The related condition reads:

$$\max(y_\mathrm{U}, y_\mathrm{V}) < y_0 \quad ; \qquad \min(y_\mathrm{U}, y_\mathrm{V}) > y_0 \quad ; \tag{7}$$

which holds in the case under discussion, keeping in mind $y_\mathrm{U} < y_\mathrm{V} < y_0$ with no loss of generality, as shown in Fig. 1.

Taking the logarithm on both sides of Eq. (6) yields:

$$\gamma \ln \frac{x_\mathrm{V}}{x_\mathrm{U}} = \ln \ln \frac{C_1 - y_0 + y_\mathrm{V}}{C_1} - \ln \ln \frac{C_1 - y_0 + y_\mathrm{U}}{C_1} \quad ; \tag{8}$$

where U = A; V = B, C; with no loss of generality. The cross product of related equations reads:

$$\begin{aligned} &\ln \frac{x_\mathrm{C}}{x_\mathrm{A}} \left[\ln \ln \frac{C_1 - y_0 + y_\mathrm{B}}{C_1} - \ln \ln \frac{C_1 - y_0 + y_\mathrm{A}}{C_1} \right] \\ &= \ln \frac{x_\mathrm{B}}{x_\mathrm{A}} \left[\ln \ln \frac{C_1 - y_0 + y_\mathrm{C}}{C_1} - \ln \ln \frac{C_1 - y_0 + y_\mathrm{A}}{C_1} \right] \quad ; \end{aligned} \tag{9}$$

which, in particular, can be solved for the crossing points, $(0, y_0)$, $(x_\mathrm{A}, y_\mathrm{A})$, $(1, y_\mathrm{B})$, $(2, y_\mathrm{C})$, where $x_\mathrm{B} = 1$, $x_\mathrm{C} = 2$, for convenience.

The intersection between the curve on the left and right-hand side of Eq. (9) yields the value of C_1. The value of C_3 can be readily inferred from Eq. (2) as:

$$C_3 = y_0 - C_1 \quad ; \tag{10}$$

and the value of C_2 is determined via particularization of Eq. (3) to $(1, y_\mathrm{B})$. The result is:

$$C_2 = \ln \frac{C_1}{C_1 - y_0 + y_\mathrm{B}} \quad ; \tag{11}$$

finally, γ is determined via particularization of Eq. (8) to U = A; V = B, C. The result is:

$$\gamma = \left(\ln \frac{x_\mathrm{B}}{x_\mathrm{C}}\right)^{-1} \left[\ln\ln \frac{C_1 - y_0 + y_\mathrm{C}}{C_1} - \ln\ln \frac{C_1 - y_0 + y_\mathrm{B}}{C_1}\right] \quad ; \tag{12}$$

where $x_\mathrm{B}/x_\mathrm{C} = 1/2$ in the case under discussion.

With regard to interpolation curves related to selected stellar initial metallicities, the expression of the mathematical variables, (x, y), in terms of the physical variables, $[\log(m/m_\odot), \log(\tau/\mathrm{y})]$, is constrained by the domain of the interpolation curve, defined by Eq. (1), $x \ge 0$, which implies the following:

$$x = \log\left(\frac{m}{m_\odot}\right) - \log\left(\frac{m_0}{m_\odot}\right) \quad ; \qquad y = \log\left(\frac{\tau}{\mathrm{y}}\right) \quad ; \tag{13}$$

where m_0 is the sample star exhibiting the lowest mass i.e. the longest lifetime, $m_0/m_\odot = 0.6$ in the case under discussion [14]. The crossing points can be explicitly expressed as: $\mathsf{P}_0 \equiv [0, \log(\tau_{0.6}/\mathrm{y})]$, $\mathsf{P}_\mathrm{A} \equiv [-\log 0.6, \log(\tau_{1.0}/\mathrm{y})]$, $\mathsf{P}_\mathrm{B} \equiv [1, \log(\tau_{6.0}/\mathrm{y})]$, $\mathsf{P}_\mathrm{C} \equiv [2, \log(\tau_{60.0}/\mathrm{y})]$, where $\tau_{m/m_\odot}$ is the lifetime of a star with selected initial metallicity and initial mass equal to m in solar units.

With regard to interpolation curves related to ordinates of crossing points averaged over the whole set of stellar initial metallicity, the expression of the mathematical variables, (x, y), in terms of the physical variables, $[\log(m/m_\odot), \overline{\log(\tau/\mathrm{y})}]$, for the abscissa, x, is provided by Eq. (13), while the ordinate, y, reads:

$$y = \overline{\log\left(\frac{\tau}{\mathrm{y}}\right)} = \frac{1}{5}\sum_{i=1}^{5} \log\left(\frac{\tau}{\mathrm{y}}\right)_{Z_i} \quad ; \tag{14}$$

where Z_i, $1 \le i \le 5$, are the stellar initial metallicities for which stellar evolution has been computed [14]. The crossing points can be explicitly expressed as: $\mathsf{P}_0 \equiv [0, \overline{\log(\tau_{0.6}/\mathrm{y})}]$, $\mathsf{P}_\mathrm{A} \equiv [-\log 0.6, \overline{\log(\tau_{1.0}/\mathrm{y})}]$, $\mathsf{P}_\mathrm{B} \equiv [1, \overline{\log(\tau_{6.0}/\mathrm{y})}]$, $\mathsf{P}_\mathrm{C} \equiv [2, \overline{\log(\tau_{60.0}/\mathrm{y})}]$.

Within the stellar initial mass range under consideration, $0.6 \le m/m_\odot \le 120.0$, the stellar lifetime range reads $6 < \log(\tau/\mathrm{y}) < 11$, which implies $y \gg 0$ via Eqs. (13) and (14). Accordingly, use can be made of the relative errors:

$$R(y) = 1 - \frac{y_\mathrm{fit}}{y} \quad ; \tag{15}$$

where y is inferred from computer output via Eq. (13) or (14), and y_fit is the counterpart of y on the related interpolation curve. The results are fitted to a good extent provided relative errors maintain small enough, within a few percent say.

Table 1: Parameters (p) of the interpolated $\log(m/m_\odot)$-$\log(\tau/\mathrm{y})$ relation, C_1, C_2, C_3, γ, for selected stellar initial metallicities, $Z = Z_1$-Z_5 with regard to cases (c) 1-5, and for ordinates of crossing points averaged over the whole set of stellar initial metallicity, case 6, with the addition of the special choice, $\gamma = 1$, leaving the remaining parameters unchanged, case 7. See text for further details.

p: c	Z	C_1	C_2	C_3	γ
1	Z_1	5.10551	0.785151	5.52594	0.96950
2	Z_2	5.23694	0.784218	5.49141	0.96686
3	Z_3	5.20510	0.824914	5.60580	0.98915
4	Z_4	5.08428	0.904558	5.81444	1.03125
5	Z_5	4.92130	0.995420	5.93483	1.05302
6	$\bar{Z}$	5.07899	0.862584	5.70612	1.00322
7	$\bar{Z}$	5.07899	0.862584	5.70612	1

3 Results

With regard to selected stellar initial metallicities, the interpolated $\log(m/m_\odot)$-$\log(\tau/\mathrm{y})$ relation is plotted in Fig. 1 as full curves, which exhibit negligible difference with the exception of the supersolar stellar initial metallicity, $Z = Z_5$, where slightly lower values are shown. A dotted horizontal line, $\log(\tau/\mathrm{y}) = 8$, marks a conventional boundary between long-lived (up) and short-lived (down) stars, which could be of interest for simple chemical evolution models (e.g., [6], [13]) and type Ia supernova progenitor models (e.g., [1]).

The parameters of the interpolated $\log(m/m_\odot)$-$\log(\tau/\mathrm{y})$ relation, C_1, C_2, C_3, γ, are listed in Table 1. The parameters lie within narrow ranges, namely $4.92 < C_1 < 5.24$; $0.78 < C_2 < 1.00$; $5.49 < C_3 < 5.71$; $0.96 < \gamma < 1.06$. The special case, $\gamma = 1$, makes the interpolation curve reduce from a double power-law (an exponential whose argument is, in turn, a power) to a simple exponential. The interpolation curve related to averaged ordinates of crossing points and its reduction to a simple exponential, cases 6 and 7 of Table 1, are plotted in Fig. 1 as a dashed and a dotted curve, respectively.

The relative errors, $R(y)$, defined by Eq. (15), as a function of the logarithmic stellar initial mass, $\log(m/m_\odot)$, are plotted in Fig. 2 for interpolation curves related to both selected stellar initial metallicities, cases 1-5 of Table 1 (top panel) and averaged ordinates of crossing points, cases 6-7 of Table 1 (bottom panel), where different symbols are captioned as in Fig. 1. An inspection of Fig. 2 shows the relative errors do not exceed about 2% in the former alternative and less than 4% in the latter one. Then it may safely be thought interpolation curves, expressed by Eq. (1), with values of parameters listed in Table 1, satisfactorily fit to the computed $\log(\tau/\mathrm{y})$-$\log(m/m_\odot)$ relation.

The special case, $\gamma = 1$, deserves further attention in that the interpolation curve reduces to a simple exponential via Eq. (1), as:

$$y = C_1 \exp(-C_2 x) + C_3 \quad ; \tag{16}$$

and the substitution of Eq. (13) into (16) after some algebra yields:

$$\log\left(\frac{\tau}{\mathrm{y}}\right) = C_1' \left(\frac{m}{m_\odot}\right)^{-C_2'} + C_3 \quad ; \tag{17}$$

$$C_1' = C_1 \exp\left[C_2 \log\left(\frac{m_0}{m_\odot}\right)\right] \quad ; \qquad \frac{m_0}{m_\odot} = 0.6 \quad ; \qquad C_2' = \frac{C_2}{\ln 10} \quad ; \tag{18}$$

which implies stellar lifetime is expressed by a double power-law, more specifically an exponential whose argument is, in turn, a power, as:

$$\frac{\tau}{\mathrm{y}} = \exp_{10}\left[C_1' \left(\frac{m}{m_\odot}\right)^{-C_2'} + C_3\right] \quad ; \tag{19}$$

where the parameter values are:

$$C_1' = 4.19439 \quad ; \qquad C_2' = 0.374616 \quad ; \qquad C_3 = 5.70612 \quad ; \tag{20}$$

according to case 7 listed in Table 1.

4 A simple application

With regard to a single star generation, let the stellar initial mass function be a power-law as:

$$\phi\left(\frac{m}{m_\odot}\right) = A\left(\frac{m}{m_\odot}\right)^p \quad ; \tag{21}$$

where A is the star formation efficiency and $-3 \le p \le -2$ for the cases of interest, in particular $p = -2.35$ relates to a classical investigation on the solar neighbourhood [18].

By definition, $\mathrm{d}N = \phi(m/m_\odot)\,\mathrm{d}(m/m_\odot)$ is the number of stars born within the mass range, $m/m_\odot \mp \mathrm{d}(m/m_\odot)/2$, and the initial mass of the star generation reads:

$$M^*(0) = A m_\odot \int_{m_{\mathrm{mf}}/m_\odot}^{m_{\mathrm{Mf}}/m_\odot} \frac{m}{m_\odot}\left(\frac{m}{m_\odot}\right)^p \mathrm{d}\frac{m}{m_\odot} \quad ; \tag{22}$$

where $m_{\rm Mf}$ and $m_{\rm mf}$ are the upper and lower stellar initial mass limit, respectively, in solar units.

The mass of the star generation (without stellar remnants) at the time, $t=\tau(m/m_\odot)$, reads:

$$M^*\left(\frac{\tau}{\rm y}\right)=Am_\odot\int_{m_{\rm mf}/m_\odot}^{m/m_\odot}\frac{m}{m_\odot}\left(\frac{m}{m_\odot}\right)^p{\rm d}\frac{m}{m_\odot}\quad; \tag{23}$$

where $\tau(m/m_\odot)$ is the lifetime of a star of initial mass m in solar units.

The fractional mass of the star generation, $s(\tau/{\rm y})=M^*(\tau/{\rm y})/M^*(0)$, can be determined from Eqs. (22) and (23) after performing integration. The result is:

$$s\left(\frac{\tau}{\rm y}\right)=\frac{(m/m_\odot)^{2+p}-(m_{\rm mf}/m_\odot)^{2+p}}{(m_{\rm Mf}/m_\odot)^{2+p}-(m_{\rm mf}/m_\odot)^{2+p}}\quad;\qquad p\ne-2\quad; \tag{24a}$$

$$s\left(\frac{\tau}{\rm y}\right)=\frac{\ln(m/m_{\rm mf})}{\ln(m_{\rm Mf}/m_{\rm mf})}\quad;\qquad p=-2\quad; \tag{24b}$$

regardless of the star formation efficiency.

The fractional mass of a star generation, expressed by Eq. (24), is plotted in Fig. 3 for $p=-3.0,-2.9,...,-2.0$, from top to bottom, with regard to the interpolation curve expressed by a simple exponential, Eq. (16), case 7 of Table 1. Related stellar lifetimes, corresponding to the whole range for which stellar evolution has been computed in the parent paper [14], are marked by dotted vertical lines where $m_{\rm mf}/m_\odot=0.6$ and $m_{\rm Mf}/m_\odot=120.0$. A restricted number of stellar initial masses are captioned on the top of the box.

An inspection of Fig. 3 shows the expected trend: mild stellar initial mass functions ($p \lesssim -2$) imply a larger fraction of short-lived stars and, in turn, a change in star mass fraction at a decreasing rate. On the other hand, steep stellar initial mass functions ($p \gtrsim -3$) imply a larger fraction of long-lived stars and, in turn, a change in star mass fraction at an increasing rate. Interestingly, the transition case where the $s(\tau/{\rm y})$-$\log(\tau/{\rm y})$ relation is linear, is close to the Salpeter's value, $p=p_{\rm lin}\approx-2.35$.

To gain more insight, the above mentioned special case relates to a straight line passing through the points, $[\log(\tau_{\rm mf}/{\rm y}),0]$ and $[\log(\tau_{\rm Mf}/{\rm y}),1]$, which can be expressed as:

$$s\left(\frac{\tau}{\rm y}\right)=\frac{\log(\tau/{\rm y})-\log(\tau_{\rm mf}/{\rm y})}{\log(\tau_{\rm Mf}/{\rm y})-\log(\tau_{\rm mf}/{\rm y})}\quad; \tag{25}$$

where $\tau_{\rm mf}=\tau(m_{\rm mf})$, $\tau_{\rm Mf}=\tau(m_{\rm Mf})$, for brevity. The combination of Eqs. (24a) and (25), after little algebra, yields:

$$\log\left(\frac{\tau}{\rm y}\right)=\frac{\log(\tau_{\rm Mf}/{\rm y})-\log(\tau_{\rm mf}/{\rm y})}{(m_{\rm Mf}/m_\odot)^{2+p}-(m_{\rm mf}/m_\odot)^{2+p}}\left(\frac{m}{m_\odot}\right)^{2+p}$$

$$- \frac{\log(\tau_{\mathrm{Mf}}/\mathrm{y}) - \log(\tau_{\mathrm{mf}}/\mathrm{y})}{(m_{\mathrm{Mf}}/m_\odot)^{2+p} - (m_{\mathrm{mf}}/m_\odot)^{2+p}} \left(\frac{m_{\mathrm{mf}}}{m_\odot}\right)^{2+p} + \log\left(\frac{\tau_{\mathrm{mf}}}{\mathrm{y}}\right) \quad ; \qquad (26)$$

where $p = p_{\mathrm{lin}}$ via Eq. (25).

The comparison of Eq. (26) with (17) term by term implies the validity of the following relations:

$$C'_2 = -2 - p \quad ; \qquad (27)$$

$$C'_1 = \frac{\log(\tau_{\mathrm{Mf}}/\mathrm{y}) - \log(\tau_{\mathrm{mf}}/\mathrm{y})}{(m_{\mathrm{Mf}}/m_\odot)^{2+p} - (m_{\mathrm{mf}}/m_\odot)^{2+p}} \quad ; \qquad (28)$$

$$C_3 = - \frac{\log(\tau_{\mathrm{Mf}}/\mathrm{y}) - \log(\tau_{\mathrm{mf}}/\mathrm{y})}{(m_{\mathrm{Mf}}/m_\odot)^{2+p} - (m_{\mathrm{mf}}/m_\odot)^{2+p}} \left(\frac{m_{\mathrm{mf}}}{m_\odot}\right)^{2+p} + \log\left(\frac{\tau_{\mathrm{mf}}}{\mathrm{y}}\right) \quad ; \qquad (29)$$

where, in the case under discussion, the left-hand side of Eqs. (27)-(29) is known via Eq. (20) and $m_{\mathrm{mf}} = 0.6$, $m_{\mathrm{Mf}} = 120.0$. Then $p = p_{\mathrm{lin}}$ can be evaluated via Eqs. (20), (27), and Eqs. (28) and (29) are merely to be verified. The result is:

$$p_{\mathrm{lin}} = -2.374616 \quad ; \qquad (30)$$

where the values of C'_1 and C_3 coincide with their counterparts expressed by Eq. (20), as expected.

In conclusion, a star generation where the initial mass function is expressed by a power-law within the range, $0.6 \le m/m_\odot \le 120.0$, implies a linear dependence of the star mass fraction, $s(\tau/\mathrm{y})$, on the logarithmic stellar lifetime, $\log(\tau/\mathrm{y})$, for an exponent of the initial mass function close to Salpeter's value, $p_{\mathrm{lin}} \approx -2.35$.

5 Discussion and conclusion

Computed stellar $\log(\tau/\mathrm{y})$-$\log(m/m_\odot)$ relations are interpolated to a good extent by double power-laws and, in particular, by a single power-law, Eqs. (1) and (16), respectively, regardless of the initial stellar metallicity, within the stellar initial mass range, $0.6 \le m/m_\odot \le 120.0$. The case of a single power-law is expecially attractive due to its simplicity over an extended mass domain.

By comparison, a $\log(\tau/\mathrm{y})$-$\log(m/m_\odot)$ relation can be used for massive ($m/m_\odot > 6.6$) stars (e.g., [11]), while a cumbersome expression is necessary for less massive stars (e.g., [16]). In alternative, four different $\log(\tau/\mathrm{y})$-$\log(m/m_\odot)$ relations can be used within the mass range, $1.3 \le m/m_\odot \le 120.0$ [10]. A three-parameter (depending on the stellar initial metallicity) fit to earlier results from the Padua group [2], [4], [5] is restricted to $Z \le 0.03$ and the extrapolation does not reproduce the correct trend as $m/m_\odot \to +\infty$ [15].

Table 2: Comparison between computed stellar lifetimes [14], τ_{Pa98}, and their counterparts inferred from the single power-law interpolation curve, case 7 of Table 1, τ_7, outside the domain towards high-mass stars. See text for further details.

$m/m_\odot$	$\tau_{\mathrm{Pa98}}/\mathrm{y}$	τ_7/y
150	3.0E6	2.2286E6
200	2.7E6	1.9162E6
300	2.5E6	1.5894E6
500	2.0E6	1.3032E6
1000	2.0E6	1.0507E6
$+\infty$		5.7061E5

With regard to the interpolation curve, expressed by Eq. (16), the following relations hold for stellar initial masses outside the domain of computed stellar evolution [14] used in the current attempt:

$$\log\left(\frac{\tau_0}{\mathrm{y}}\right) \to +\infty \quad ; \qquad \frac{m}{m_\odot} \to 0 \quad ; \tag{31}$$

$$\log\left(\frac{\tau_\infty}{\mathrm{y}}\right) = C_3 = 5.70612 \quad ; \qquad \frac{m}{m_\odot} \to +\infty \quad ; \tag{32}$$

which is the correct trend, in the sense that (failed) stars with mass, $m/m_\odot < m_{\mathrm{mf}}/m_\odot \approx 0.08$, never start hydrogen burning and related lifetime can be conceived as infinite. On the other hand, stars with increasingly high mass exhibit finite lifetime regardless of initial metallicity. The comparison between computed lifetimes [14] and their counterparts inferred from the interpolation curve, expressed by Eqs. (16), (20), case 7 of Table 1, is shown in Table 2. It is apparent lifetimes calculated via the single power-law interpolation curve outside the domain towards high stellar masses are understimated with respect to computed values, by a factor not exceeding 2 up to $m/m_\odot = 1000$.

Concerning stars with decreasingly low mass, a similar comparison is shown in Table 3, where computed stellar lifetimes are from a different source [9], restricted to stellar initial metallicity, $Z = 0.02$ [8]. It is apparent lifetimes calculated via the single power-law interpolation curve outside the domain towards low stellar masses are unacceptably overestimated with respect to computed values but, interestingly, the discrepancy is within the same order of magnitude for $m/m_\odot = 0.25$, where stellar evolution still attains the giant phase [9]. Accordingly, an absence of the giant phase would imply a different $\log(\tau/\mathrm{y})$-$\log(m/m_\odot)$ relation.

A simple but acceptable linear fit to the results listed in Table 3, leaving

Table 3: Comparison between computed stellar lifetimes [9], τ_{La97}, and their counterparts inferred from the single power-law interpolation curve, case 7 of Table 1, τ_7, outside the domain towards low-mass stars. See text for further details.

$m/m_\odot$	$\tau_{\mathrm{La97}}/\mathrm{y}$	τ_7/y
0.08	1.1E13	3.24E16
0.10	6.2E12	4.40E15
0.12	4.2E12	9.72E14
0.14	3.4E12	2.93E14
0.16	2.7E12	1.10E14
0.18	2.0E12	4.78E13
0.20	1.8E12	2.35E13
0.25	1.7E12	5.71E12

aside $m/m_\odot = 0.25$, reads:

$$\log\left(\frac{\tau}{\mathrm{y}}\right) = -2\log\left(\frac{m}{m_\odot}\right) + 10.8 \quad ; \tag{33}$$

which implies $\log(\tau_{1.0}/\mathrm{y}) = 10.800$ and $\log(\tau_{0.6}/\mathrm{y}) = 11.257$, larger but of about the same order of magnitude with respect to their counterparts determined from stellar evolution [14].

The computed $\log(\tau/\mathrm{y})$-$\log(m/m_\odot)$ relation, represented in Fig. 1, extended to the results listed in Tables 2 and 3, is shown in Fig. 4 where, in addition, the single power-law interpolation curve and the interpolation line, Eqs. (16), (20), and (33), respectively, are also plotted together with the asymptotic limit of the interpolation curve for infinite stellar initial mass. The global trend exhibited by the computed $\log(\tau/\mathrm{y})$-$\log(m/m_\odot)$ relation is reminiscent of earlier results restricted to stellar initial metallicity, $Z = 0.02$ [10], where the transition between two different regimes occurs above (e.g., [19]) instead of below (Fig. 4) the solar mass.

In conclusion, the single power-law interpolation curve, expressed by Eqs. (16), (20), can safely be extrapolated towards high-mass stars ($m/m_\odot > 120.0$) yielding understimated values within a factor of two up to $m/m_\odot = 1000$ and within a fiducial factor of four up to $m/m_\odot \to +\infty$. Additional caution must be used for the extrapolation towards low-mass stars ($m/m_\odot < 0.6$), yielding overstimated values within a factor of about three down to $m/m_\odot = 0.25$ and to unacceptably larger overstimates down to $m/m_\odot = 0.08$.

The question if the single power-law interpolation curve, expressed by Eqs. (16), (20), arises from a mere coincidence or has a theoretical interpretation, is outside the aim of the current attempt but some considerations can be performed. Differentiating both sides of Eq. (16), after little algebra yields:

$$\frac{\mathrm{d}\not\tau}{\mathrm{d}\not m} = -\lambda \not m^{-\beta} \not\tau \quad ; \tag{34}$$

$$\not\tau = \frac{\tau}{\mathrm{y}} \quad ; \qquad \not m = \frac{m}{m_\odot} \qquad \lambda = C_1' C_2' \quad ; \qquad \beta = C_2' + 1 \quad ; \tag{35}$$

where the special case, $\beta = 0$, reduces to the equation of the exponential decay, $\not\tau$ being related to the number of decaying nuclides and $\not m$ to the time. Accordingly, Eq. (34) learns (i) longer stellar lifetimes imply larger change of stellar lifetime with stellar initial mass and vice versa, and (ii) higher stellar initial masses imply lower change of stellar lifetime with stellar initial mass and vice versa. In the author's opinion, a theoretical explanation of Eq. (16) should necessarily start from the above mentioned points.

The fractional stellar mass as a function of the logarithmic stellar lifetime, shown in Fig. 3, relates to a single star generation and to a power-law stellar initial mass function, which are limiting cases. In reality, multiple star generations appear even in low-mass stellar systems and the stellar initial mass function exhibits a more complex trend with respect to a simple power-law. On the other hand, the ideal situation depicted in Fig. 3 is expected to show a similar trend with respect to the real case, at least for environments where the whole amount of pristine gas was turned into stars in a short time, less than 1 Gyr say, such as the inner halo, the thick disk, and globular clusters. It is worth noticing the stellar mass is less than the total mass, in that the contribution of stellar remnants (white dwarfs, neutron stars, black holes) and baryonic dark matter is neglected: in any case, the related contribution is expected to be of a few percent at most.

With regard to globular clusters with age equal to $\tau_{0.9}$ (first vertical line on the right of $\log(\tau/\mathrm{y}) = 10$), an inspection of Fig. 3 shows a present star mass fraction, $0.07 \lesssim s \lesssim 0.35$, according if $-2 \ge p \ge -3$, in particular $s \approx 0.15$ for the Salpeter's exponent, $p = -2.35$, close to a linear dependence of the star mass fraction on the logarithmic stellar lifetime. Then a mild stellar initial mass function, $p \approx -2.1$, implies an initial mass larger by a factor of about ten, for globular clusters with age equal to $\tau_{0.9}$, in the case under consideration.

The main results of the current note can be summarized as follows.

(1) The computed $\log(\tau/\mathrm{y})$-$\log(m/m_\odot)$ relation for the stellar initial mass range, $0.6 \le m/m_\odot \le 120.0$, and the stellar initial metallicity range, $0.0004 \le Z \le 0.0500$, tabulated in an earlier attempt [14] is fitted to a good extent by a double power-law for assigned initial metallicity, which can be reduced to a single power-law for the whole set of initial metallicities. The relative errors, $R[\log(\tau/\mathrm{y})] = 1 - \log(\tau_{\mathrm{fit}}/\mathrm{y})/\log(\tau/\mathrm{y})$, do not exceed about 2% for the double power-law and 4% for the single power-law.

(2) The interpolation curve, expressed by a single power-law, can be extrapolated towards both high-mass and low-mass stars. In the former alternative, stellar lifetimes are understimated by a factor less than 2 up to $m/m_\odot = 1000$ [14] and by a fiducial factor less than 4 up to $m/m_\odot \to +\infty$. In the latter alternative, stellar lifetimes are overstimated by a factor less than about 3 down to $m/m_\odot = 0.25$ and by an unacceptably large factor down to $m/m_\odot = 0.08$ [9].

(3) The first derivative, $\mathrm{d}(\tau/\mathrm{y})/\,\mathrm{d}(m/m_\odot)$, related to the single power-law interpolation curve, is a generalization of the equation of the exponential decay, which could be the starting point for a theoretical interpretation of the $\log(\tau/\mathrm{y})$-$\log(m/m_\odot)$ relation.

(4) In the special case of a single star generation with stellar initial mass function defined by a power-law, using the single power-law interpolation curve within the mass range, $0.6 \le m/m_\odot \le 120.0$, the star mass fraction declines in time at a decreasing rate for mild stellar initial mass function ($p \lesssim -2$) and at an increasing rate for steep stellar initial mass function ($p \gtrsim -3$), where a linear trend is exhibited for a value of the exponent close to the Salpeter's value ($p_{\mathrm{lin}} \approx -2.35$).

Acknowledgement

Thanks are due to C. Chiosi for useful discussions.

References

[1] I. A. Acharova, B. K. Gibson, Yu. N. Mishurov, V. V. Kovtyukh, Galactic constraints on supernova progenitor models, Astronomy & Astrophysics, 557 (2013), A107, 1-9. http://dx.doi.org/10.1051/0004-6361/201220944

[2] M. Alongi, G. Bertelli, A. Bressan, et al., Evolutionary sequences of stellar models with semiconvection and convective overshoot. I - Z = 0.008, Astronomy & Astrophysics Supplement Series, 97 (1993), 851-871.

[3] M. Asplund, N. Grevesse, A. J. Sauval, P. Scott, The Chemical Composition of the Sun, Annual Review of Astronomy and Astrophysics, 47 (2009), 481-522. http://dx.doi.org/10.1146/annurev.astro.46.060407.145222

[4] G. Bertelli, A. Bressan, C.Chiosi, F. Fagotto, E. Nasi, Theoretical isochrones from models with new radiative opacities, Astronomy & Astrophysics Supplement Series, 106 (1994), 275-302.

[5] A. Bressan, F. Fagotto, G. Bertelli, C. Chiosi, Evolutionary sequences of stellar models with new radiative opacities. II - Z = 0.02, Astronomy & Astrophysics Supplement Series, 100 (1993), 647-664.

[6] R. Caimmi, A Simple Multistage Closed-(Box+Reservoir) Model of Chemical Evolution, Serbian Astronomical Journal, 183 (2011), 37-61. http://dx.doi.org/10.2298/saj1183037c

[7] R. Caimmi, Self-Consistency and Continuity Questions on Axisymmetric, Rigidly Rotating Polytropes, Applied Mathematical Sciences, 8 (2014), 6039-6079. http://dx.doi.org/10.12988/ams.2014.48602

[8] G. Laughlin , P. Bodenheimer, Luminosity functions for very low mass stars and brown dwarfs, Astrophysical Journal, 403 (1993), 303-314. http://dx.doi.org/10.1086/172203

[9] G. Laughlin, P. Bodenheimer, F. C. Adams, The End of the Main Sequence, Astrophysical Journal, 482 (1997), 420-432. http://dx.doi.org/10.1086/304125

[10] A. Maeder G. Meynet, Grids of evolutionary models from 0.85 to 120 solar masses - Observational tests and the mass limits, Astronomy & Astrophysics, 210 (1989), 155-173.

[11] F. Matteucci, L. Greggio, Relative roles of type I and II supernovae in the chemical enrichment of the interstellar gas, Astronomy & Astrophysics, 154 (1986), 279-287.

[12] P. Padovani, F. Matteucci, Stellar Mass Loss in Elliptical Galaxies and the Fueling of Active Galactic Nuclei, Astrophysical Journal, 416 (1993), 26-35. http://dx.doi.org/10.1086/173212

[13] B. E. J. Pagel, B. E. Patchett, Metal abundances in nearby stars and the chemical history of the solar neighborhood, Monthly Notices of the Royal Astronomical Society, 172 (1975), 13-40. http://dx.doi.org/10.1093/mnras/172.1.13

[14] L. Portinari, C. Chiosi, A. Bressan, Galactic chemical enrichment with new metallicity dependent stellar yields, Astronomy & Astrophysics, 334 (1998), 505-539.

[15] C.M. Raiteri, M. Villata, J.E. Navarro, Simulations of Galactic chemical evolution. I. O and Fe abundances in a simple collapse model, Astronomy & Astrophysics, 315 (1996), 105-115.

[16] A. Renzini, A. Buzzoni, Global properties of stellar populations and the spectral evolution of galaxies, in Spectral Evolution of Galaxies, ed. C. Chiosi and A. Renzini (Dordrecht: Reidel), (1986), 195-235. http://dx.doi.org/10.1007/978-94-009-4598-2_19

[17] D. Romano, C. Chiappini, F. Matteucci, M. Tosi, Quantifying the uncertainties of chemical evolution studies. I. Stellar lifetimes and initial mass function, Astronomy & Astrophysics, 430 (2005), 491-505. http://dx.doi.org/10.1051/0004-6361:20048222

[18] E. E. Salpeter, The Luminosity Function and Stellar Evolution, Astrophysical Journal, 121 (1955), 161-167. http://dx.doi.org/10.1086/145971

[19] R. P. C. Wiersma, J. Schaye, T. Theuns, C. Dalla Vecchia, L. Tornatore, Chemical enrichment in cosmological, smoothed particle hydrodynamics simulations, Monthly Notices of the Royal Astronomical Society, 399 (2009), 574-600. http://dx.doi.org/10.1111/j.1365-2966.2009.15331.x

Received: January 13, 2015; Published: February 23, 2015

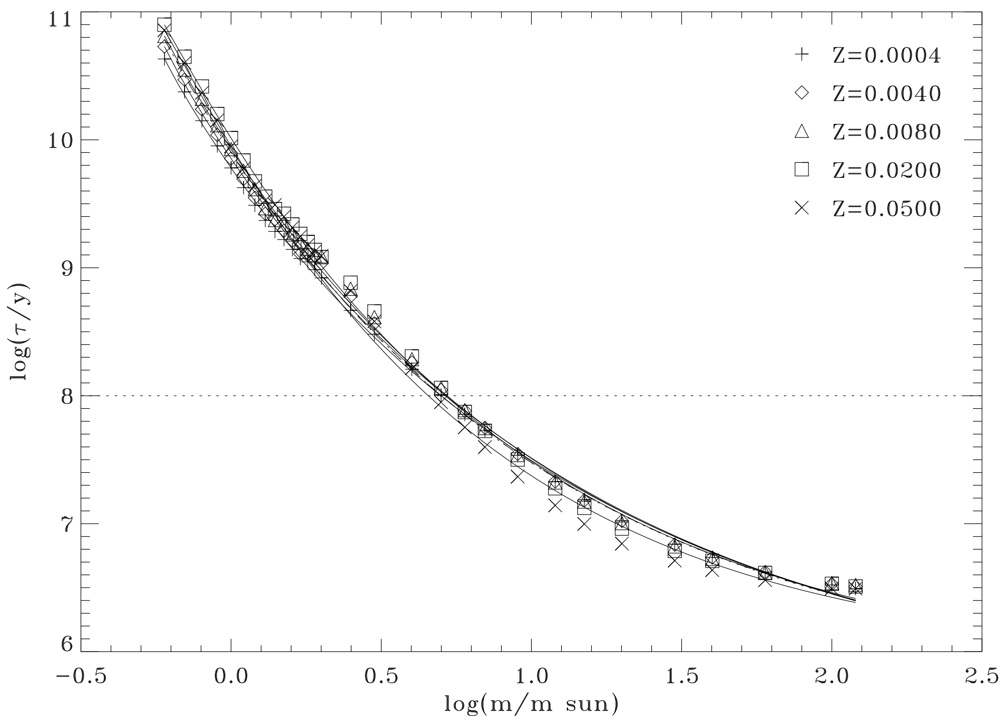

Figure 1: Computed $\log(\tau/\mathrm{y})$-$\log(m/m_\odot)$ relation for 30 different stellar initial masses within the range, $0.6 \leq m/m_\odot \leq 120.0$, in connection with 5 different stellar initial metallicities [14]. Different symbols relate to different metallicities as indicated. Four-parameter interpolation curves are shown as full for selected stellar initial metallicity; dashed for ordinates of crossing points averaged over the whole set of stellar initial metallicity; dotted for parameters, C_1, C_2, C_3, as in the last case and γ set equal to unity. The dotted horizontal line marks a conventional boundary between long-lived (top) and short-lived (bottom) stars. See text for further details.

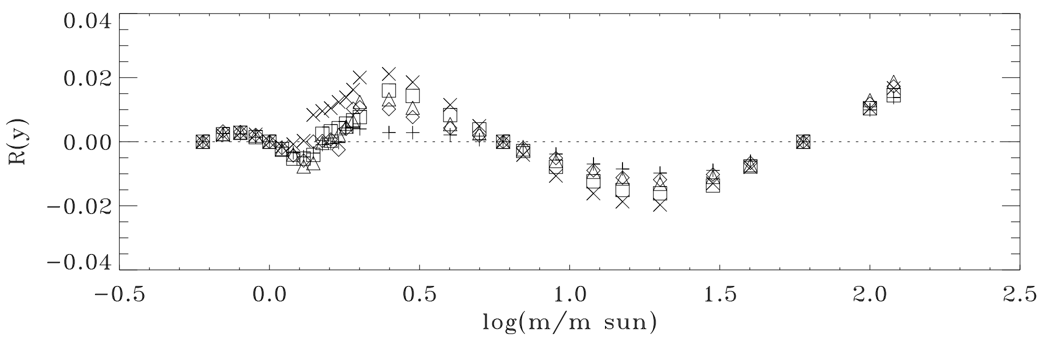

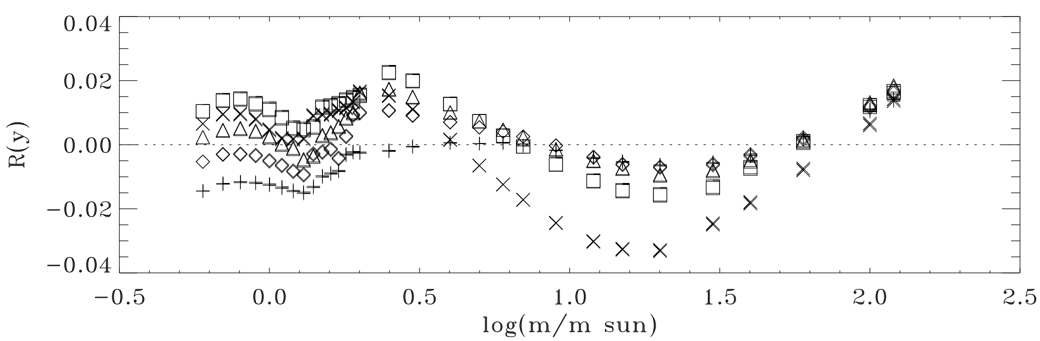

Figure 2: The relative error, $R(y) = 1 - \log(\tau_{\rm fit}/\mathrm{y})/\log(\tau/\mathrm{y})$, as a function of the logarithmic stellar initial mass, $\log(m/m_\odot)$, with regard to interpolation curves related to selected stellar initial metallicity (top panel) and to averaged ordinates of crossing points (bottom panel). Different symbols correspond to different stellar initial metallicity as shown in Fig. 1. See text for further details.

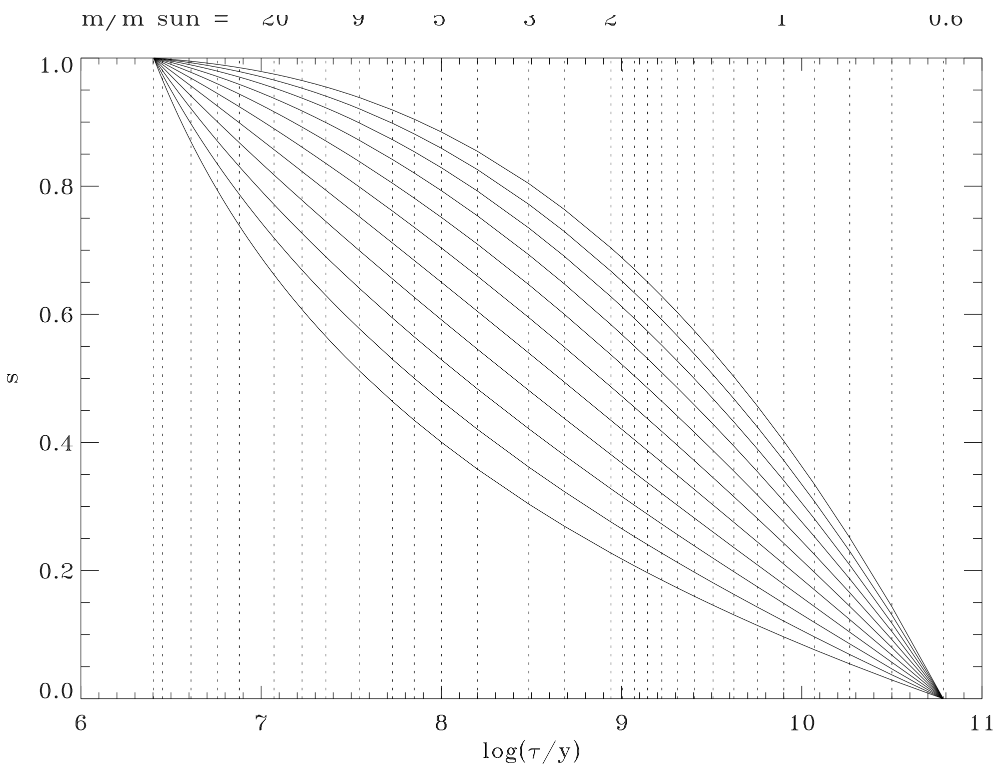

Figure 3: Fractional mass of a star generation, $s(\tau/\mathrm{y}) = M^*(\tau/\mathrm{y})/M^*(0)$, as a function of the logarithmic stellar lifetime, $\log(\tau/\mathrm{y})$, for a power-law stellar initial mass function with exponent equal to (from top to bottom) $p = -3.0, -2.9, ..., -2.0$, with regard to a computed $\log(\tau/\mathrm{y})$-$\log(m/m_\odot)$ relation interpolated by a simple exponential, restricted to the domain, $0.6 \leq m/m_\odot \leq 120.0$. Related stellar lifetimes, corresponding to the whole range for which stellar evolution has been computed [14], are marked by dotted vertical lines, a restricted number of which are captioned on the top of the box.

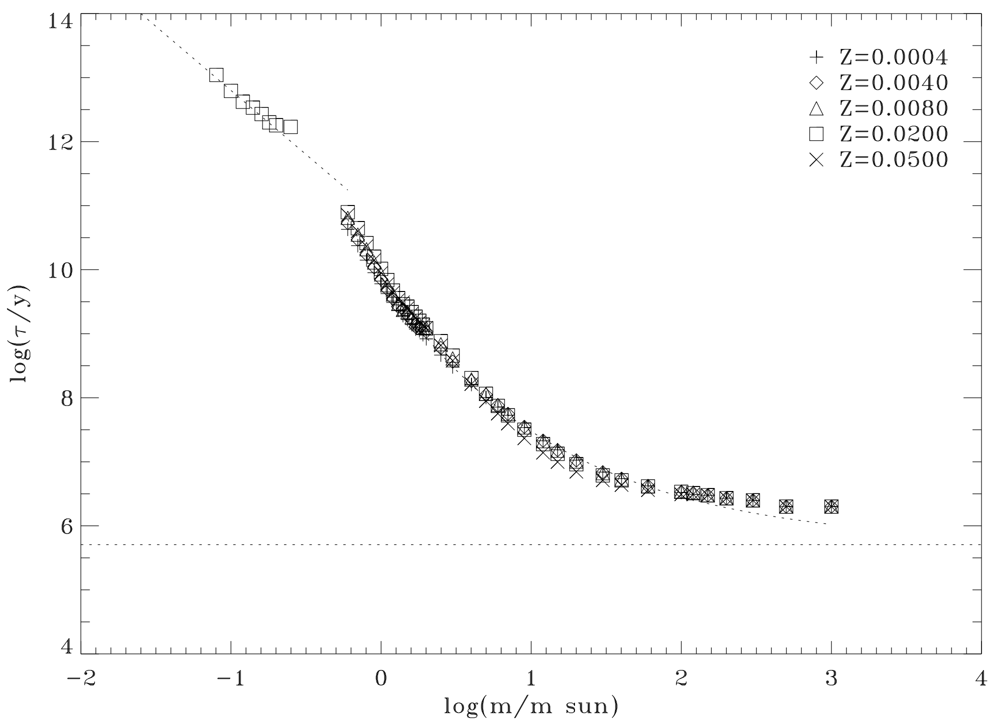

Figure 4: Computed log(τ/y)-log($m/m_\odot$) relation, plotted in Fig. 1, extended to both lower [9] and larger [14] stellar initial masses. Lower masses relate to stellar initial metallicities, $Z = 0.02$. An interpolation straight line and power-law curve, respectively, are also shown (dotted). The asymptotic limit of the interpolation curve towards infinite stellar initial mass is marked by a dotted horizontal line. See text for further details.